AN EXTENDED ANALYSIS OF DIFFUSION FLAMES WITH FUEL DROPLETS IN THE REACTION ZONE

Luciano Hennemann, hennemann@lcp.inpe.br
Fernando F. Fachini, fachini@lcp.inpe.br

Laboratório de Combustão e Propulsão - LCP
Instituto Nacional de Pesquisas Espaciais - INPE
12630-000, Cachoeira Paulista, SP, Brazil

Abstract. *This work presents an extended analysis of the external structure of diffusion flames established with reactant (ethanol as fuel and oxygen as oxidant) in counterflow configuration. This model assumes part of fuel in liquid phase (droplets) dispersed in the gas phase and is also considered that the droplets are not completely consumed at the flame and thus they coexist in the oxidant side. In the literature, the counterflow diffusion flame model is called flamelet. Following the same nomenclature, the counterflow diffusion flame with droplets is called spraylet. The mathematical description of this spraylet is made by the conservation equations with source terms. In the fuel species conservation equation, the extra term is a source which has a strength proportional to the droplets vaporization rate. On the other hand, in the oxidant conservation equation the extra term takes into account the stoichiometric consumption proportional to the droplets vaporization rate. In the energy conservation equation, two extra terms appear: one is a sink which has a strength proportional to the product of the droplet vaporization rate and the latent heat, and the second one is a source proportional to the droplet burning in the oxidant side. In this extended analysis, the flame stability with droplets escaping by the flame is studied and good agreement for the flame position and flame temperature are obtained analytically. The results point out the conditions to find stable flames.*

Keywords: *flamelet, spraylet, droplet, diffusion flame.*

1. INTRODUCTION

Spray combustion is present in many devices, from rocket motor to house heating. The main target of the atomization is to increase the surface area between the liquid and gas phases to achieve high rates of evaporation. In order to do it, the jet or sheet of liquid is transformed in small droplets by processes that depends of the disruption of the surface tension of the liquid by aerodynamic forces, or an external mechanical energy applied through rotating or vibrating devices. In the absence of these forces, the liquid tends to form a single sphere because the surface tension present.

When the liquid atomization in a ambient gas occurs, a number of mechanisms occur until we obtain a final spectrum of droplets. The aerodynamic pressure profile around the droplets contributes for the deformation because it changes the equilibrium state of the droplet and also the surface tension and viscosity. This allow the breaking of the droplet or further deformations. Three types of deformation can occur: the droplet becomes flattened forming a oblate ellipsoid, and so this form is converted in torus disintegrating into small droplets, initial droplets are elongated forming a long cylinder or ligament breaking into small droplets, local deformations on surface that creates bulges or protuberances will broke forming new droplets. So any particular preference for a type of deformation and breakup depends on physics properties of the gas and liquid employed, viscosities, densities, interfacial tension and the ambient around the droplet [Lefebvre 1989, Sirignano 1999]. For liquids with low viscosity, the deformation is determined by the Weber number which relates the aerodynamic force with the surface tension. For small Weber numbers, the droplet is flattened, initially forming a pancake shape and then becoming thin as a membrane. The membrane divides into very small droplets and larger droplets is formed from the edges. For a large number of Weber, the droplet is deformed uniformly and fibers or filaments are formed on its surface resulting stable droplets [Faeth 1995]. Atmospheric conditions and the low viscosity of the liquid when exposed at high velocity airstream, may block the breaking of the droplet. So, different critical Weber numbers are estimated, in order to be used for these cases. The Ohnesorge [Ohnesorge 1936] number relates the viscous forces with the strength of surface tension. It is used in spray technology in conjunction with Reynolds and Weber numbers, to map schemes formation of droplets.

Sprays are more dense in the first layers after the injection and more rarefied as it moves away of these layers beyond the liquid surface. In the downstream direction, the dense spray gradually evolves into a dilute spray [Faeth 1983, Sirignano 1999]. In the dense part, the influence of the velocity profile on the liquid jet or sheet disintegration can be explained briefly. The growth of the axisymmetric surface oscillations of the jet or sheet, causes the Rayleigh jet breakup [Rayleigh 1878] and the droplets diameter exceed the jet orifice diameter. The primary droplets breakup is unstable and occurs near the liquid jet surface. The relative velocity between the jet and the ambient gas increases the surface tension producing a distribution of static pressure through the jet or sheet, accelerating the collapse. The breaking of the droplets occurs to many diameters ahead of the jet. The droplets have the same jet diameter. The second breakup contributes with

the final droplets sizes and its distribution. The droplets are produced by the growth of short surface waves on the unstable surface of the jet caused by the relative motion between the jet and ambient gas. This growth of the wave is opposed to the surface tension. The droplets are broken at a distance of several diameters beyond the eject orifice. The diameters of the droplets formed are much smaller than the diameter of the jet. In the dilute region, the atomization is concluded and only droplets with size much smaller than the orifice of the jet are present [Lefebvre 1989].

The turbulence generated by the liquid injection is not a determining factor in the deceleration and deformation of droplets but also promotes random behavior and spread of droplets in the gaseous medium. In the same way, the momentum transferred between gas and liquid will modulate the turbulence level within the gas phase. This process was reviewed by Faeth [Faeth 1983] and should be taking into account the number of Stokes which relates the relaxation time (time required for the droplet reaches the final velocity) and the eddy lifetime. With small Stokes number (less than 1), small particles are trapped within the eddies following the vortex structure. As the Stokes number equal to 1, centrifugal forces act on the droplet but no trap in the eddy and when the Stokes number is greater than 1, the trajectories of the particles remain unchanged [Stiesch 2003].

When one considers spray combustion, heat transfer must be taken into account from the flame to the droplets. The transferred heat from ambient to a cold droplet surface divides in: part of the heat is used to gasify the droplet and the other part is transferred to the droplet center to heating it up [Faeth 1983]. The liquid mass is converted to vapor and dispersed to ambient. Heat and mass diffusion are the control rate of the process. We consider droplets sufficiently far apart, such that there is no interaction between them. This level of interaction is one of the three possibility ones, as explained by Sirignano [Sirignano 1999].

In combustion processes of a droplet and consequently a spray occurs through the establishment of a turbulent diffusion flame where fuel and oxidant are present in the reaction zone. Thus, the flamelet model employs the idea of dividing a turbulent flame in small sections. So the flamelet behavior is considered with laminar combustion and can be treated as a one-dimensional process depending only on the rate of mixing between gaseous fuel and oxidant. The model spraylet which is used here only distinguishes itself by having droplets present in the reaction zone. Diffusion flames cover various configurations and one of the most used is the counterflow. This configuration is also widely used in theoretical and numerical methods [Continillo and Sirignano 1990, Li 1997]. The advantages that the model presents are the stability, well defined flow field and ease of implementation of experimental boundary conditions such as, strain rate, temperature, composition, supply of fuel and oxidizer [Gutheil and Sirignano 1998]. Numerical simulations were performed using Eulerian and Lagrangian formulation for droplet drag and vaporization. Watanabe et. al. [Watanabe et al. 2007] made a study with two-phase combustion exploring the properties of spray fuel in a laminar counterflow. They examined effects such strain rate, equivalent ratio, droplets size in terms of mixture fraction and scalar rate. Large differences in the trends were found among the spray flame and the gaseous diffusion flame in respect of mass fractions of chemical species, gas temperature and scalar dissipation rate. The temperature of the spray flames becomes much higher than gaseous diffusion flame due to the lower scalar dissipation rate and also when premixed and diffusion combustion occurs simultaneously in the spray flame. Continillo and Sirignano [Continillo and Sirignano 1990] obtained a similar numerical solution for a planar counterflow spray flame where air, droplets and inert gas were considered. Transient heating and vaporization of droplets were obtained with this solution. They observed that two distinct flame zones with both premixed-like and diffusion-like characteristics were founded for some configurations. The separation of the flame into a premixed flame zone and a diffusion flame is caused by the increase of the initial droplet diameter. The separation is inhibited when the strain rate increases making the flame more compact.

Liñán [Liñán 1974] made a theoretical study and used a counterflow model in order to make an asymptotic analysis on structures of diffusion flame for large activation energies. He also investigated ignition and extinction conditions, analyzing the behavior of the temperature and the *Damköhler* number for the regimes: nearly frozen, partial burning, premixed flame and near-equilibrium diffusion flame.

In a previous work was used the model proposed by Liñán considering part of the fuel in the liquid phase without droplets escaping by the flame. The aim of this extended work is to analyse counterflowing spray flames where droplets escape to the oxidizer side. New terms were included in the energy and species conservation equations to simulate it. The *Schvab-Zeldovich* formulation is used to combine the governing equations in order to eliminate the non linear *Arrhenius* term and a one step reaction mechanism is considered [Continillo and Sirignano 1990, Greenberg and Sarig 1996]. An analysis is performed for the outer zone and the behavior of the flame position and temperature, changing the fuel mass fraction injected is shown.

This work is organized as follows. The first section contain all the formulation adopted. The second section presents the solution obtained to the model. The third section shows the main results and the last presents our conclusions.

2. FORMULATION

The flow geometry is composed by two opposite flows. The gaseous fuel comes through the left stream and the gaseous oxidant comes from the right stream. The flame stabilizes near the plane that contains the stagnation point. We will admit in this work fuel partially in liquid phase to simulate the spray combustion. The injection of the liquid fuel

occurs near the flame, in order to find fuel in liquid phase inside the flame (see Fig. 1).

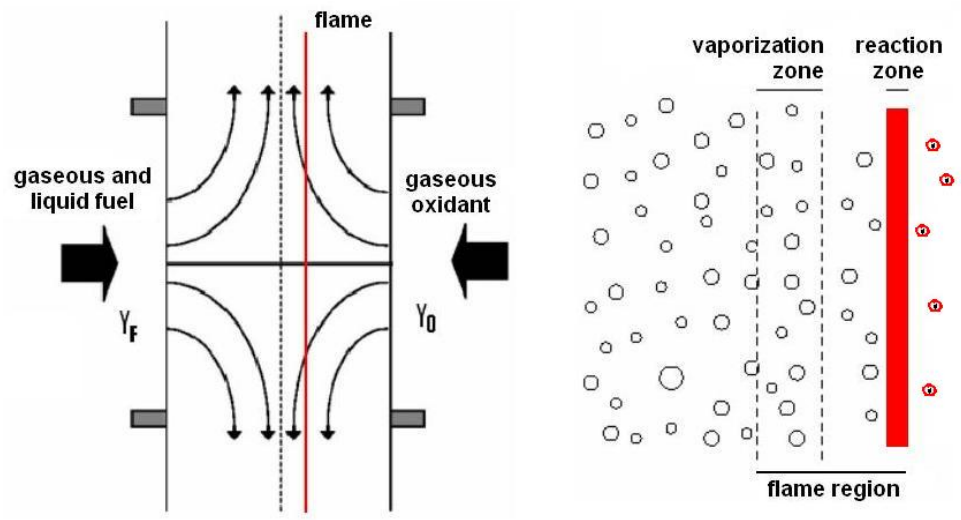

Figure 1. Spraylet model adopted and droplets in the flame region.

Because of the presence of the liquid in this problem, the conservation equations will have sink and source terms. For the oxidant conservation equation, the extra term inserted takes into account the stoichiometric consumption proportional to the droplets vaporization rate. For the fuel species conservation equation, the source term is determined by the distribution of the number of droplets per volume multiplied by the mass vaporization rate. For the energy conservation equation, the sink term in the fuel side is determined by the distribution of the number of droplets per volume multiplied by the mass vaporization rate and the latent heat. Likewise in the oxidant side, a source term proportional to the droplet burning is introduced. A heaviside function H_s is inserted defining the location of the droplets in the fuel or oxidizer side. The following set of equations describes the fuel and oxidant mass fractions and the temperature of the flow,

$$\bar{\rho}\bar{u}\,\frac{\partial}{\partial\bar{z}}\left\{\begin{array}{c}\bar{Y}_O\\ \bar{Y}_F\\ \bar{h}\end{array}\right\}=\frac{\partial}{\partial\bar{z}}\left(\left\{\begin{array}{c}\bar{\rho}\,\bar{D}_O\\ \bar{\rho}\,\bar{D}_F\\ \bar{K}\end{array}\right\}\frac{\partial}{\partial\bar{z}}\left\{\begin{array}{c}\bar{Y}_O\\ \bar{Y}_F\\ \bar{T}\end{array}\right\}\right)+\left\{\begin{array}{c}-\bar{\nu}\\ -1\\ \bar{Q}\end{array}\right\}\bar{W}+\left\{\begin{array}{c}-\bar{\nu}\bar{N}\dot{\bar{m}}H_s\\ \bar{N}\,\dot{\bar{m}}H_s^*\\ -\bar{N}\,\dot{\bar{m}}\,\bar{l}H_s^*+\bar{N}\dot{\bar{m}}(\bar{Q}-\bar{l})H_s\end{array}\right\}. \quad (1)$$

Here we have four terms that mean; the first one a convective term, the second term is a diffusive term, the third term is the chemical reaction and the last one, source and sink terms were included. Note that the heaviside function H_s is defined as

$$H_s(x-x_f)=\left\{\begin{array}{l}1,\ \text{if}\ x>x_f\\ 0,\ \text{if}\ x<x_f,\end{array}\right. \quad (2)$$

and H_s^* is the image of H_s being defined as

$$H_s^*=\left\{\begin{array}{l}0,\ \text{if}\ x>x_f\\ 1,\ \text{if}\ x<x_f.\end{array}\right. \quad (3)$$

The variables that have an overwritten bar will be transformed on non dimensional units using these boundary conditions

$$\left\{\begin{array}{l}\bar{z}=-\infty,\ \bar{Y}_F=Y_{F-\infty},\ \bar{T}=\bar{T}_{-\infty},\ \bar{Y}_O=0,\ \bar{\rho}=\bar{\rho}_{-\infty}\\ \bar{z}=+\infty,\ \bar{Y}_O=Y_{O+\infty},\ \bar{T}=\bar{T}_{+\infty},\ \bar{Y}_F=0,\ \bar{\rho}=\bar{\rho}_{+\infty}.\end{array}\right. \quad (4)$$

Since the flame is close to the stagnation point, the flow velocity is approximated by $\bar{u}=-A\bar{z}$. So, we shall use this following non dimensional variables: the mixing layer $z\equiv\bar{z}/\bar{l}_c$, the oxidant mas fraction $y_O\equiv\bar{Y}_O/\bar{\nu}Y_{F-\infty}$, where $\bar{\nu}$ is stoichiometric mass ratio, fuel mass fraction $y_F\equiv\bar{Y}_F/Y_{F-\infty}$, the temperature $T\equiv c_p\bar{T}/\bar{Q}Y_{F-\infty}$ with specific heat c_p and heat release $\bar{Q}$, the density $\rho=\bar{\rho}/\bar{\rho}_c$, where $\bar{\rho}_c=\rho_{+\infty}$, the velocity $u=\bar{u}/\bar{u}_c$, where $\bar{u}_c=A\bar{l}_c$. Note that the characteristic length $\bar{l}_c$ is determined by $\bar{K}/\bar{\rho}_c c_p A\bar{l}_c^2=1$, where $\bar{K}$ is thermal conductivity. The source term is composed by $\bar{N}$, that is the number os droplets of fuel, the property $\bar{l}$ is the latent heat needed to evaporate the mass of droplet and $\dot{m}$ is the rate of mass vaporized and depends on the latent heat supplied.

The properties are

$$W\equiv\frac{\bar{W}\bar{l}_c}{Y_{F_{-\infty}}\bar{u}_c\bar{\rho}_c};\ \ Q\equiv\frac{\bar{Q}}{\bar{Q}Y_{F_{-\infty}}};\ \ N\dot{m}\equiv\frac{\bar{N}\dot{\bar{m}}\bar{l}_c}{Y_{F-\infty}\,\bar{u}_c\bar{\rho}_c}; \quad (5)$$

$$N\dot{m}l \equiv \frac{\bar{N}\dot{\bar{m}}\bar{l}\bar{l}_c}{\bar{Q}Y_{F-\infty}\bar{u}_c\bar{\rho}_c};\;\; N\dot{m}(Q-l) \equiv \frac{\bar{N}\dot{\bar{m}}\bar{l}_c(\bar{Q}-\bar{l})}{\bar{Q}Y_{F-\infty}\bar{u}_c\bar{\rho}_c};\;\; l \equiv \frac{\bar{l}}{\bar{Q}}; \tag{6}$$

$$\bar{l}_c \equiv \sqrt{\frac{D_{OF}}{A}};\;\; D_F = D_O = \frac{\bar{K}}{\bar{\rho}_c c_p};\;\; \frac{\bar{K}}{\bar{\rho}_c c_p A\bar{l}_c^2} \equiv 1;\;\; L_{eF} = L_{eO} = 1. \tag{7}$$

Here D_O and D_F are the diffusion coefficients for oxidant and fuel and W is the molecular weight. Remember that in the problem, the normalized oxidant mass fraction leads to $\alpha^{-1} = \nu Y_{F-\infty}/Y_{O+\infty}$, which is called equivalence ratio.

In this analysis we assume for simplicity that the thermodynamic and transport coefficients are constant. The energy and species conservation equations in the non dimensional form are [Liñán 1974]:

$$\frac{d^2T}{dz^2} + z\frac{dT}{dz} = -Dy_o y_F e^{-T_a/T} + N\dot{m}lH_s^* - N\dot{m}(1-l)H_s \tag{8}$$

$$\frac{d^2y_F}{dz^2} + z\frac{dy_F}{dz} = Dy_o y_F e^{-T_a/T} - N\,\dot{m}H_s^* \tag{9}$$

$$\frac{d^2y_o}{dz^2} + z\frac{dy_o}{dz} = Dy_o y_F e^{-T_a/T} + N\dot{m}H_s. \tag{10}$$

which satisfies the boundary conditions

$$\begin{cases} z \to -\infty,\;\; y_O = 0,\;\; y_F = 1,\;\; T = T_{-\infty} \\ z \to +\infty,\;\; y_O = \alpha,\;\; y_F = 0,\;\; T = T_{+\infty}. \end{cases} \tag{11}$$

Note that T_a is the non dimensional activation energy of the *Arrhenius* term. The *Schvab-Zeldovich* procedure is applied to reduce the number of equations. The resulting equations describe the functions $H \equiv (T + ly_F)/(1-l) + y_O$ and $Z \equiv y_F - y_O$, which are known in the literature as excess of enthalpy and mixture fraction respectively

$$\frac{d^2H}{dz^2} + z\frac{dH}{dz} = 0 \tag{12}$$

$$\frac{d^2Z}{dz^2} + z\frac{dZ}{dz} = -N\dot{m}H_s^* - N\dot{m}H_s. \tag{13}$$

3. SOLUTION

Physically, the liquid fuel in droplet form arrives from one side of the flame and the oxidant arrives from the other side, and so, these flows are opposed in the viscous layer with fuel droplets leakage through the flame. The droplets are released at a certain distance and the gaseous fuel stream pushes them to the flame. The conservation equations are defined from $z \to -\infty$ to $z \to +\infty$ but they are described in a more convenient way from 0 to 1, using

$$x = \frac{1}{2}\text{erfc}(\frac{z}{\sqrt{2}}), \tag{14}$$

which is the solution of the homogeneous (12). By performing the transformation from z to x on Eq. (12) and (13) one finds

$$\frac{d^2H}{dx^2} = 0, \tag{15}$$

$$\frac{d^2Z}{dx^2} = 2\pi e^{z^2}[-N\dot{m}H_s^* - N\dot{m}H_s], \tag{16}$$

recalling that $H \equiv (T + ly_F)/(1-l) + y_O$ and $Z \equiv y_F - y_O$ and satisfy

$$\begin{cases} x = 0,\;\; H = (T_{-\infty} + l)/(1-l);\;\; Z = 1 \\ x = 1,\;\; H = T_{+\infty}/(1-l) + \alpha;\;\; Z = -\alpha. \end{cases} \tag{17}$$

The solution of Eq. (15) with the boundary conditions from Eq. (17) is

$$\frac{1}{1-l}(T + ly_F) + y_O = \frac{1}{1-l}(T_{-\infty} + l) + \left[\frac{1}{1-l}(\beta - l) + \alpha\right]x, \tag{18}$$

where $\beta \equiv T_{+\infty} - T_{-\infty}$ [Liñán 1974]. By applying the condition on the flame, $y_F = y_O = 0$, $T = T_e$ at $x = x_e$, the flame temperature is found from Eq. (18)

$$T_e = T_{-\infty} + l + [\beta - l + \alpha(1-l)]x_e. \tag{19}$$

By observing Eq. (19), the flame temperature T_e is a function of the flame position x_e. Thus an extra expression relating T_e and x_e is necessary to solve the problem. In the fuel side of the flame, the source term $N\dot{m}$ determines the fuel entering in the gas phase domain by the vaporization of the cloud of droplets. The present work admits that the vaporization rate distribution is similar to a *Gaussian Distribution*, $N\dot{m} \equiv (\bar{M}/2\pi)e^{-(z^2-z_i^2)}$. For the distribution, Eq. (16) with the boundary condition Eq. (17) presents an analytical solution,

$$Z = y_F = -Mx^2 + \left(\frac{Mx_e^2 - 1}{x_e}\right)x + 1, \tag{20}$$

and the boundary conditions that are satisfies $Z = 1$ at $x = 0$ and $Z = 0$ at $x = x_e$. Note that $M \equiv (\bar{M}/2)e^{z_i^2}$. In the oxidant side of the flame the source term is the same, thus the solution of Eq. (16) with the boundary condition Eq. (17) and $Z = 0$ at the flame $x = x_e$ is

$$Z = y_O = Mx^2 - \left(\frac{M - \alpha - Mx_e^2}{1 - x_e}\right)x + \left(\frac{M - \alpha - Mx_e^2}{1 - x_e}\right)x_e - Mx_e^2. \tag{21}$$

The next step is to define the position of the flame x_e, which is still unknown. As the flame is small, the functions on both sides remain the same obtaining continuity through the flame

$$\frac{d^2y_F}{dx^2} = 2\pi e^{z^2}[-N\dot{m}H_s^*] \text{ for } 0 \le x \le x_e \tag{22}$$

$$\frac{d^2y_O}{dx^2} = 2\pi e^{z^2}[-N\dot{m}H_s] \text{ for } x_e \le x \le 1. \tag{23}$$

For this distribution, the solution of Eq. (16) uses the boundary conditions Eq. (17) and $Z = 0$ at the flame $x = x_e$. Considered as being very close to the flame, the flame position x_e is obtained by the stoichiometric flow

$$\left.\frac{dy_F}{dx}\right|_{x_e^-} = -\left.\frac{dy_O}{dx}\right|_{x_e^+}, \tag{24}$$

and by imposing the condition of Eq. (24) on Eq. (20) and (21), we determine the flame position x_e

$$Mx_e^2 + x_e(\alpha - M + 1) - 1 = 0. \tag{25}$$

4. RESULTS

In this present work, ethanol (C_2H_6OH) is the simulated fuel and oxygen is the oxidant. The considered properties are: the heat combustion $Q = 27899\ kJ/kg$ [Avallone and Baumeister 1987], the latent heat $l = 846\ kJ/kg$ [Turns 2000], the specific heat $c_p(medium) = 1.947\ kJ/kgK$ [Turns 2000] and the ambient temperature is $T_{+\infty} = T_{-\infty} = 300\ K$, consequently $\beta = 0$. The stoichiometric mass coefficient is $\nu = 2.0869$ based on one-step chemical kinetics

$$C_2H_6O + 3O_2 \rightarrow 2CO_2 + 3H_2O. \tag{26}$$

We present temperature and mass fractions profiles for different value of the parameter α. Also we show the influence of the intensity of the vaporization rate in temperature and position of the flame. For all cases, the oxygen mass fraction is $Y_{O+\infty} = 1$, so that changes on α correspond to the fuel concentration changes.

Figure (2) shows mass fraction profiles for different α. Here, the vaporization rate was fixed to $M = 30$. The interval $0,87 \le x \le 0,89$ corresponds the flame position for different α adopted, which fuel and oxidant mass fraction are zero. The vaporization of the droplets is seen on the side where the fuel mass fraction increases to a maximum value. The decrease of these curves indicate that the fuel is being consumed in the flame. For the lower value α analyzed (3.25) with $(Y_{F-\infty} \sim 0.15)$ is obtained a higher amount of fuel available. It means that a large amount of fuel gas is pushing the fuel droplets to the flame. The droplets evaporate quickly when approaching the reaction zone causing a large increase in the fuel concentration. Thus, in this side occurs "saturation" with the presence of fuel in excess because there is no oxidizer enough to promote its combustion. Since a diffusion flame is established in the region where the reactants flow are in stoichiometric proportion, this low-valued α case push the flame toward the oxidant.

The temperature profile T is showed in Fig. (3) for each flame side for different α adopted using $M = 30$ also. The highest temperature for each α corresponds to the flame temperature for each case. Differently from classical counterflow

configuration where the profiles are straight lines (constant heat flux), in the present case we have curves profiles (non constant heat flux). On the fuel side the concavity of the curves is upward, indicating a decrease in the of energy (heat loss). This decrease is due to the fact that the heat is transferred to vaporize to droplets. In the oxidizer side, the slight concavity of the curves is downward indicating that energy is transferred to the ambient by droplets combustion that escaped through the flame. These remains droplets are still burning and the small fuel mass fractions in these droplets consume oxygen which is abundant in this side. The released energy of combustion causes heating of the oxidant surroundings.

The influence of the vaporization rate on the flame position is showed in Fig. (4). With the increase of vaporization rate, the amount of gaseous fuel available increases, which moves the flame towards the oxidizer in order to obtain the stoichiometric flux. The flame temperature as showed in Fig. (5) increases because in that more vaporized fuel droplets reaches the reaction zone. With a decrease of vaporization rate, we obtain liquid fuel droplets reaching to the reaction zone, removing heat from the flame and so decreasing the temperature. Despite all the α adopted, significant variations in temperature for each one is obtained. The highest flame temperature T_e obtained is (4.00) with $(Y_{F-\infty} = 0.12)$ is due to the presence of a smaller amount of gaseous fuel and thus a larger amount of droplets is burnt in the flame keeping the stoichiometric flux.

An extreme case was inserted $(\alpha = 10.00)$ to obtain the behavior in a situation where very small amount of gas fuel is imposed.

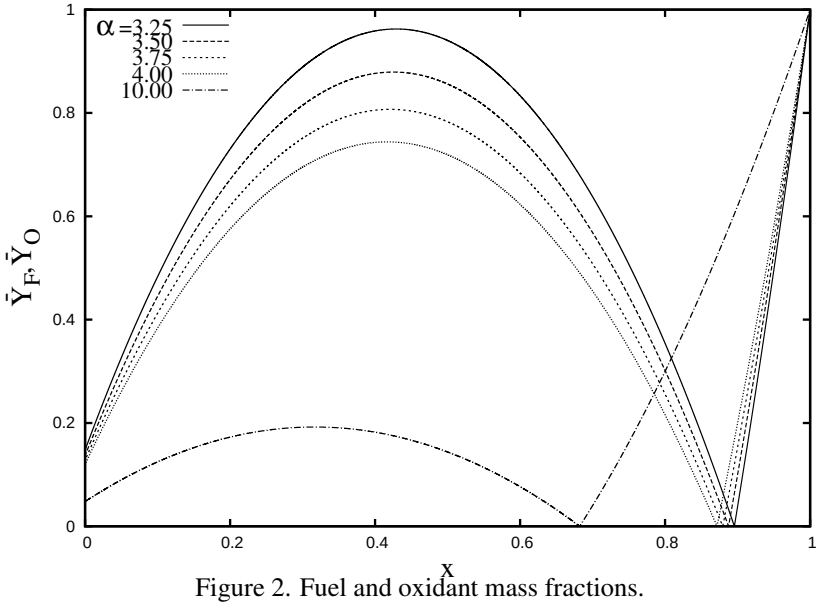

Figure 2. Fuel and oxidant mass fractions.

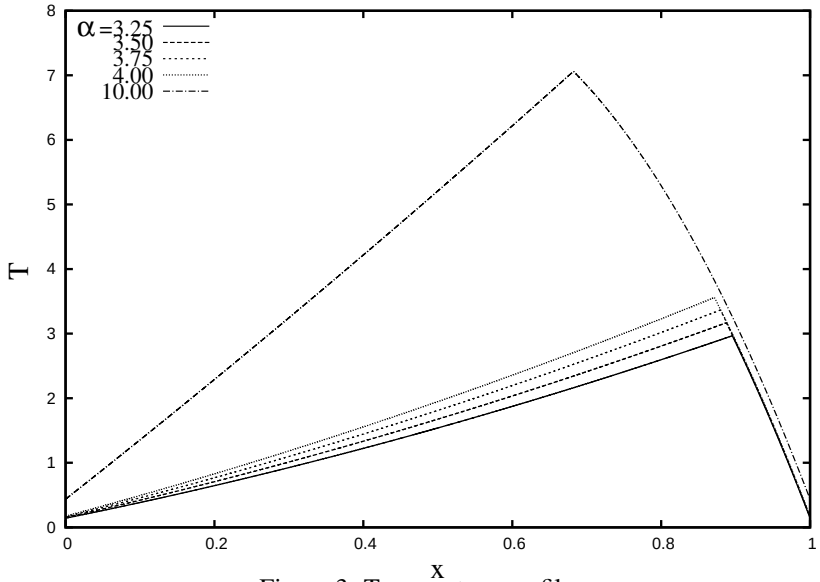

Figure 3. Temperature profile.

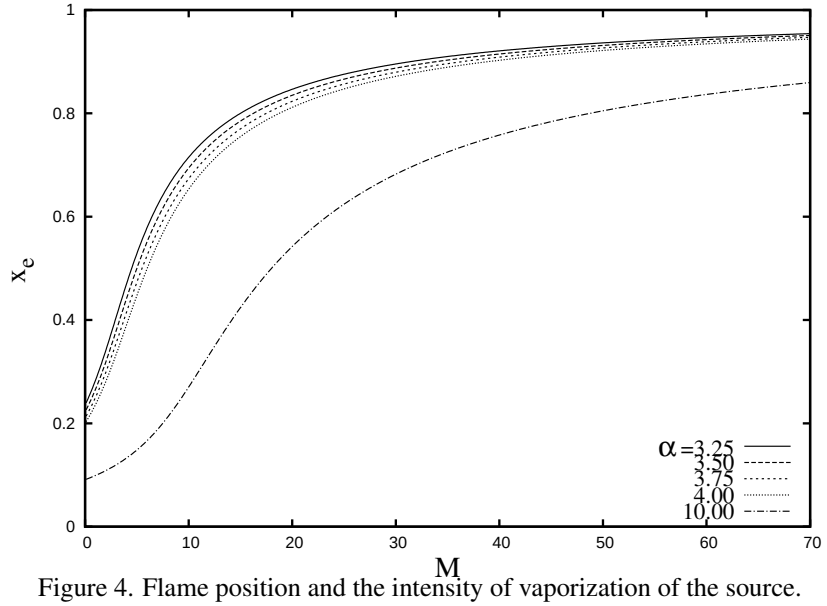

Figure 4. Flame position and the intensity of vaporization of the source.

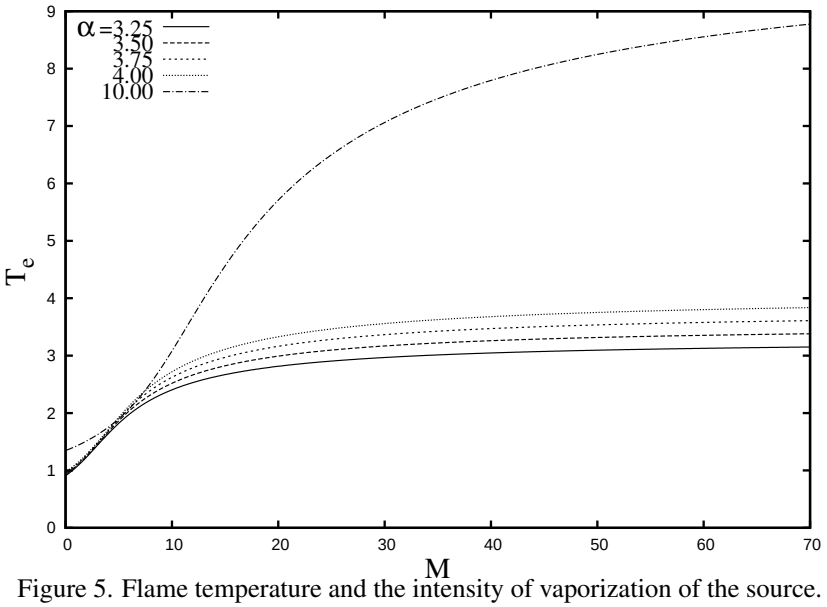

Figure 5. Flame temperature and the intensity of vaporization of the source.

5. CONCLUSION

This work presents an analysis of an external flame structure obtained from counterflowing model (the fuel and oxidant are not premixed) and considering fuel droplets mixed with gaseous fuel. This model also considers droplets escaping from the flame. These analysis are made inserting sink and source terms in the governing equations. These equations in their non dimensional forms determine the droplets vaporization rate. Analytical solutions with good agreement are obtained. An analysis of the temperature profile, as showed in Fig. (3), shows that heat is lost in the temperature side and so, this heat portion is transferred for the droplets vaporization. The heat gained on the oxidant side which is released to ambient, is obtained from the burning droplets that escaped from the flame. The mass fraction consumption is also analyzed as showed in Fig. (2).

In the same way, position and temperature of the flame are analyzed also as function of the droplets vaporization rate with different fuel concentrations in the gaseous stream as shown in Fig. (4) and Fig. (5). With a low value of α, it means high fuel concentration in gas phase mixed with fuel droplets. Thus, the flame position is pushed to the oxidizer side limit (or infinite) and the problem does not have physical meaning.

The low computational cost for calculating these properties is a motivation for to use this model in spray combustion analysis. Analysis in the internal flame structure using asymptotic theory will be performed in future work.

6. REFERENCES

Avallone, E.A., Baumeister, T., 2000, "Mark's Standart Handbook for Mechanical Engineers", McGraw-Hill, New York, USA, pp. 428.

Continillo, G., Sirignano, W.A., 1990, "Counterflow Spray Combustion Modelling", Combustion Flame, 81, pp. 325-340.

Faeth, G.M., 1983, "Evaporation and Combustion of Sprays", Prog. Energy Combust. Sci., 9, pp. 1-76.

Faeth, G.M., Hsiang, L. P., WU, P. K., 1995, "Structure and Breakup Properties of Sprays", Elsevier Science Ltd, The University of Michigan, U.S.A., 21, pp. 99-127.

Greenberg, J. B., Sarig, N., 1996, "An Analysis of Multiple Flames in Counterflow Spray Combustion", Combustion Flame, 104, pp. 431-459.

Gutheil, E. and Sirignano, W.A., 1998, "Counterflow Spray Combustion Modeling with Detailed Transport and Detailed Chemistry", Combustion Flame, 113, pp. 92-10.

Lefebvre, A.H., 1989, "Atomization and Sprays", Hemisphere: Washington, DC, USA, pp 422.

Li, S. C., 1997, "Spray Stagnation Flames", Progress in Energy and Combustion Science, 23, pp. 303-347.

Liñán, A., 1974, "The asymptotic structure of counterflow diffusion flames for large activation energies", Acta Astronautica, Vol.1, pp. 1007-1039.

Ohnesorge, W., 1936, "Formation of Drops by Nozzles and the Breakup of Liquid Jets", Z. Angew. Math. Mech., 16, pp. 355-358.

Rayleigh, Lord, 1878, "On the Instability of Jets", Proc. London Math, Soc., 10, pp. 4-13.

Sirignano, W.A., 1999, "Fluid Dynamics and Transport of Droplets and Sprays", University of California, Irvine, USA, pp. 311.

Stiesch, G., 2003, "Modelling Engine Spray and Combustion Processes", Springer Verlag Berlin Heidelberg, New York, USA, pp. 282.

Turns, S.R., 2000, "An Introduction to Combustion-Concepts and Applications", McGraw-Hill, Pennsylvania, USA, pp. 676.

Watanabe, H., Kurose, R., Hwang, S. M., Akamatsu, W., 2007, "Characteristics of flamelets in spray flames formed in a laminar counterflow", Combustion and Flame, 148, pp. 234-248.

7. RESPONSIBILITY NOTICE

The authors are the only responsible for the printed material included in this paper.